J Mater Sci: Mater Med (2010) 21:1057–1068
DOI 10.1007/s10856-009-3948-1

Properties of anti-washout-type calcium silicate bone cements containing gelatin

Chun-Cheng Chen · Meng-Heng Lai · Wei-Chung Wang · Shinn-Jyh Ding

Received: 28 July 2009 / Accepted: 16 November 2009 / Published online: 26 November 2009

Abstract Novel washout-resistant bone substitute materials consisting of gelatin-containing calcium silicate cements (CSCs) were developed. The washout resistance, setting time, diametral tensile strength (DTS), morphology, and phase composition of the hybrid cements were evaluated. The results indicated that the dominant phase of β-Ca_2SiO_4 for the SiO_2–CaO powders increased with an increase in the CaO content of the sols. After mixing with water, the setting times of the CSCs ranged from 10 to 29 min, increasing with a decrease in the amount of CaO in the sols. Addition of gelatin into the CSC significantly prolonged ($P < 0.05$) the setting time by about 2 and 8 times, respectively, for 5% and 10% gelatin. However, the presence of gelatin appreciably improved the anti-washout and brittle properties of the cements without adversely affecting mechanical strength. It was concluded that 5% gelatin-containing CSC may be useful as bioactive bone repair materials.

1 Introduction

A variety of calcium silicate-based materials, such as $CaSiO_3$ [1, 2], bioactive glass [3], and mineral trioxide aggregate [4] have been developed for use in the orthopedic and dental surgery. In a recent study, we developed a quick-setting calcium silicate cement (CSC) with high bioactivity and enhanced osteogenesis [5]. However, it could be difficult to deliver to bone defects with complex structures, and hard to compact due to the brittleness of the ceramic cement. Thus, the challenge facing such bioactive ceramic cements is susceptibility to brittle fracture. Additionally, when implanted as a paste that is just starting to set, cements tend to disintegrate upon early contact with blood or other fluids [6]. The washout resistance of the cement plays an important role in successful clinical applications. One strategy to improve the disadvantage could be the use of cohesion promoters such as cellulose, alginate, gelatin, and chitosan to modify the cements [6–12].

Naturally polymeric gelatin is obtained from bovine bone via thermal denaturation or physical and chemical degradation of collagen, and it has been widely employed as a bone graft material [9, 10] and as a drug carrier [13] because of its biocompatibility, biodegradability and non-toxicity. Bone and teeth are composite materials composed mainly of an organic matrix (collagen) and a mineral phase (hydroxyapatite) [14]. Successful design of bone substitute materials requires an appreciation for the structure of bone. Thus, the synergistic combination of organic and inorganic compounds in hybrid ceramic-polymer biomaterials makes them very useful in hard tissue repair and replacements [7–10, 15–17].

The use of a hybrid composite made of gelatin and calcium silicate, resembling the morphology and properties of natural bone, may be one way to solve the problem of ceramic brittleness and to enhance the anti-washout properties, all while maintaining good biocompatibility, high bioactivity and bonding properties. Following a previous study [5], the effect of gelatin on the properties of CSC was assessed. A series of ceramic cements with the oxide batch

C.-C. Chen · S.-J. Ding
Department of Dentistry, Chung-Shan Medical University Hospital, Taichung 402, Taiwan, Republic of China

M.-H. Lai · W.-C. Wang · S.-J. Ding (✉)
Institute of Oral Biology and Biomaterials Science, Chung-Shan Medical University, No. 110, Sec. 1, Jinguo North Road, Taichung 402, Taiwan, Republic of China
e-mail: sjding@csmu.edu.tw

formulation ranging from 60 to 30 mol% SiO_2 were prepared by the sol–gel process using tetraethyl orthosilicate and calcium nitrate as raw materials. The obtained gels and powders were characterized by thermogravimetric analysis-differential scanning calorimetry (TGA-DSC), scanning electron microscopy (SEM), and X-ray diffractometry (XRD). The purpose of the study was to examine the physicochemical properties of hybrid cements consisting of gelatin-containing calcium silicate powder as the solid phase and water as the liquid phase.

2 Materials and methods

2.1 Preparation of powders

The sol–gel method has been described elsewhere [5]. Reagent grade tetraethyl orthosilicate ($Si(OC_2H_5)_4$; TEOS, 98.0%, Sigma-Aldrich, St. Louis, MO, USA) and calcium nitrate ($Ca(NO_3)_2{\cdot}4H_2O$; 98.5%, Showa, Tokyo, Japan) were used as precursors for SiO_2 and CaO, respectively. 2 M nitric acid (HNO_3) was used as the catalyst and absolute ethanol as the solvent. The nominal molar ratios of SiO_2−CaO ranged from 6:4 to 3:7. For simplicity, throughout this study, the as-sintered powders and the cements derived from such powders were designated by the same codes. For example, the specimen code "S60C40" stands for both the as-sintered powder containing $60SiO_2$/40CaO (in mol%) and the cement derived from the powder. The general procedure of the sol–gel route, such as hydrolysis and aging, was adopted. Briefly, TEOS was hydrolyzed with the sequential addition of 2 M HNO_3 and absolute ethanol with 1 h of stirring each. The required amount of $Ca(NO_3)_2{\cdot}4H_2O$ was added to the above TEOS−HNO_3−ethanol solution and the mixed solution was stirred for an additional hour. The molar ratio of (HNO_3 + H_2O)−TEOS−ethanol was 10:1:10. The sol solution was hermetically sealed in a polypropylene bottle and placed in an oven for aging at 60°C for 1 day. After which, vaporization of the solvent in an oven at 120°C was for at least 2 days to obtain an as-dried gel.

Based on the TGA-DSC results, the as-dried gel was heated in air to 800°C at a heating rate of 10°C/min for 2 h using a high-temperature furnace and then cooled to room temperature in the furnace to produce a powder. To prepare the organic–inorganic composite, type B gelatin (isoelectric point at pH = 4.7–5.2) from bovine skin (Sigma-Aldrich, St. Louis, MO, USA) was added to the sintered powder at either 5% or 10% by weight using a conditioning mixer (ARE-250, Thinky, Tokyo, Japan). The mixtures were then ball-milled for 12 h in ethanol using a Retsch S 100 centrifugal ball mill (Hann, Germany) and dried in an oven at 60°C before use.

2.2 Characterization of the powders

After vaporization of the solvent in an oven at 120°C following aging, a Netzsch DSC 404 (Gerätebau, Germany) was used to acquire the thermal events occurring. The detection sensitivity of DSC was 0.6–16 μV/mW. Thermal stability was determined by TGA using a Seiko SSC 5000 system (Chiba, Japan) with a detection sensitivity of 0.1 μg. Both thermal analyses were started from room temperature at a heating rate of 10°C/min in air up to 1000°C. SEM (JEOL JSM-6700F, Tokyo, Japan) was used to characterize morphology of the powders and XRD (Shimadzu XD-D1, Kyoto, Japan) was used to investigate the phase composition.

2.3 Evaluation of anti-washout properties

To prepare the cement, the liquid-to-powder (L/P) ratios of 0.45, 0.5, 0.55 and 0.6 (ml/g) were adopted for the S60C40, S50C50, S40C60, and S30C70 systems, respectively. The variations in L/P depended on the Ca content because a greater amount of liquid was needed to harden the powder with the higher Ca content. The cement without gelatin was as the control. Anti-washout properties of the cement specimens were evaluated by visual observation as described by Xu et al. [18]. After mixing, the cements were molded in a stainless steel mold under a pressure of 0.7 MPa for 1 min using a uniaxial press to form the cylindrical specimen dimension of 6 mm (diameter) × 3 mm (height). This size was adopted throughout the study, unless described elsewhere. They were then taken out and immediately placed into a simulated body fluid (SBF) at 37°C. The test specimens were considered to have passed the washout resistance test if the cement did not visibly disintegrate in the solution after 1 h. The SBF solution has an ionic composition similar to that of human blood plasma. SBF consisted of 7.9949 g sodium chloride (NaCl), 0.3528 g sodium hydrogen carbonate ($NaHCO_3$), 0.2235 g potassium chloride (KCl), 0.178 g dipotassium hydrogen phosphate (K_2HPO_4), 0.305 g magnesium chloride hexahydrate ($MgCl_2{\cdot}6H_2O$), 0.2775 g calcium chloride ($CaCl_2$), and 0.071 g sodium sulfate anhydrous (Na_2SO_4) dissolved in 1000 ml of distilled H_2O and buffered to pH 7.4 with hydrochloric acid (HCl) and trishydroxymethyl aminomethane ($(CH_2OH)_3CNH_2$).

2.4 Setting time measurement

The setting times of the cements were tested using a 400-g Gillmore needle with a 1-mm diameter, in accordance with international standard ISO 9917-1 for water-based cements [19]. The setting time was defined as the point when a needle failed to create an indentation of 1 mm in depth in

three separate areas of the cement cylinder kept in 100% relative humidity at 37°C. Six parallel experiments were carried out for each group.

2.5 Phase composition and morphology of the cement

To analyze phase composition, morphology and mechanical properties of the cements, they were incubated in a 37°C and 100% humidity environment and allowed to set for 1 day. Phase analysis of the cement specimens was performed using an XRD operated at 30 kV and 30 mA at a scanning speed of 1°/min. The surfaces of the cement specimens were coated with gold using a JFC-1600 (JEOL, Tokyo, Japan) coater and examined under a JSM-6700F SEM (JEOL) operated in the lower secondary electron image (LEI) mode at 3 kV accelerating voltage.

2.6 Diametral tensile strength and modulus measurement

DTS testing was performed on an EZ-Test machine (Shimadzu, Kyoto, Japan) at a loading rate of 0.5 mm/min after the powder was mixed with water and set for 1 day in a 37°C and 100% humidity environment, as described above. The DTS value of each cement specimen was calculated using the relationship defined in the equation $DTS = 2P/\pi bw$, where P is the peak load (Newtons), b is the diameter (mm) and w is the thickness (mm) of the specimen. The maximum load at failure was obtained from the recorded load–deflection curve. The elastic modulus of the cement specimens was determined from the slope of the linear elastic portion of the load–deflection curve. At least twenty specimens from each group were tested. The interior surface (fractured surface) after diametral tensile loading was also examined by SEM.

2.7 Statistical analysis

One-way analysis of variance (ANOVA) was used to evaluate significant differences between means in the measured data. Scheffe's multiple comparison testing was used to determine the significance of standard deviations in the measured data from each specimen under different experimental conditions. In all cases, results were considered statistically significant with a P-value of less than 0.05.

3 Results

3.1 Thermal behavior of gel powders

Figure 1 shows the TGA-DSC curves of the as-dried gel powders. The four specimens showed similar thermal behavior, indicating that the first weight loss of about 10% was found, followed by continuous weight loss from 100 to 450°C in the TGA curve. The decomposition and oxidation of the decomposed products were accelerated at temperatures of 450−550°C, as evidenced by a rapid weight loss of more than 30%. In the DSC traces, there were four endothermic peaks at about 100, 520, 540, and 650°C, and one exothermic peak at about 900°C.

3.2 Powder morphology

The particle size of powders is an important characteristic, and therefore it was analyzed by SEM. In Fig. 2, the SEM micrograph shows all of the milled particles before mixing with water to essentially be an assembly of irregular particles with sizes ranging from 0.5 to 5 μm. The more CaO contents the powders contained, the smaller the particle size was. Additionally, the powers with higher SiO_2 contents presented a denser structure.

3.3 Phase composition of powders

Figure 3 shows the XRD patterns of the as-prepared SiO_2–CaO powders sintered at 800°C, indicating a phase evolution dependent on the Si/Ca molar ratio of the precursors. The major diffraction peaks at 2θ between 32 and 34° were attributed to the β-Ca_2SiO_4 (β-dicalcium silicate) phase. At higher SiO_2 content (S60C40), a broad and diffuse diffraction peak appeared. At CaO amounts greater than SiO_2 (S40C60 and S30C70) in the sol, the CaO peak at $2\theta = 37.5°$ appeared. The peak intensities of β-Ca_2SiO_4 and CaO increased with an increase in the CaO content of the starting materials.

3.4 Phase composition of cements

XRD patterns of all cements revealed an obvious diffraction peak around $2\theta = 29.4°$, corresponding to the calcium silicate hydrate (C–S–H) gel, and incompletely reacted inorganic component phases of β-Ca_2SiO_4 (Fig. 3). It is clear that the peak intensity of C–S–H formed in the gelatin-containing cement specimen was lower, in particular for 10% gelatin, when compared with the corresponding control.

3.5 Cement morphology

The SEM micrographs of the cements with and without 10% gelatin are shown in Fig. 4. The as-set CSC controls had an appearance with entangled particles and exhibited several pores. A dense structure appeared for the cement with larger CaO amounts in the sol. In contrast, when 10% gelatin was added, the organic–inorganic hybrid cements

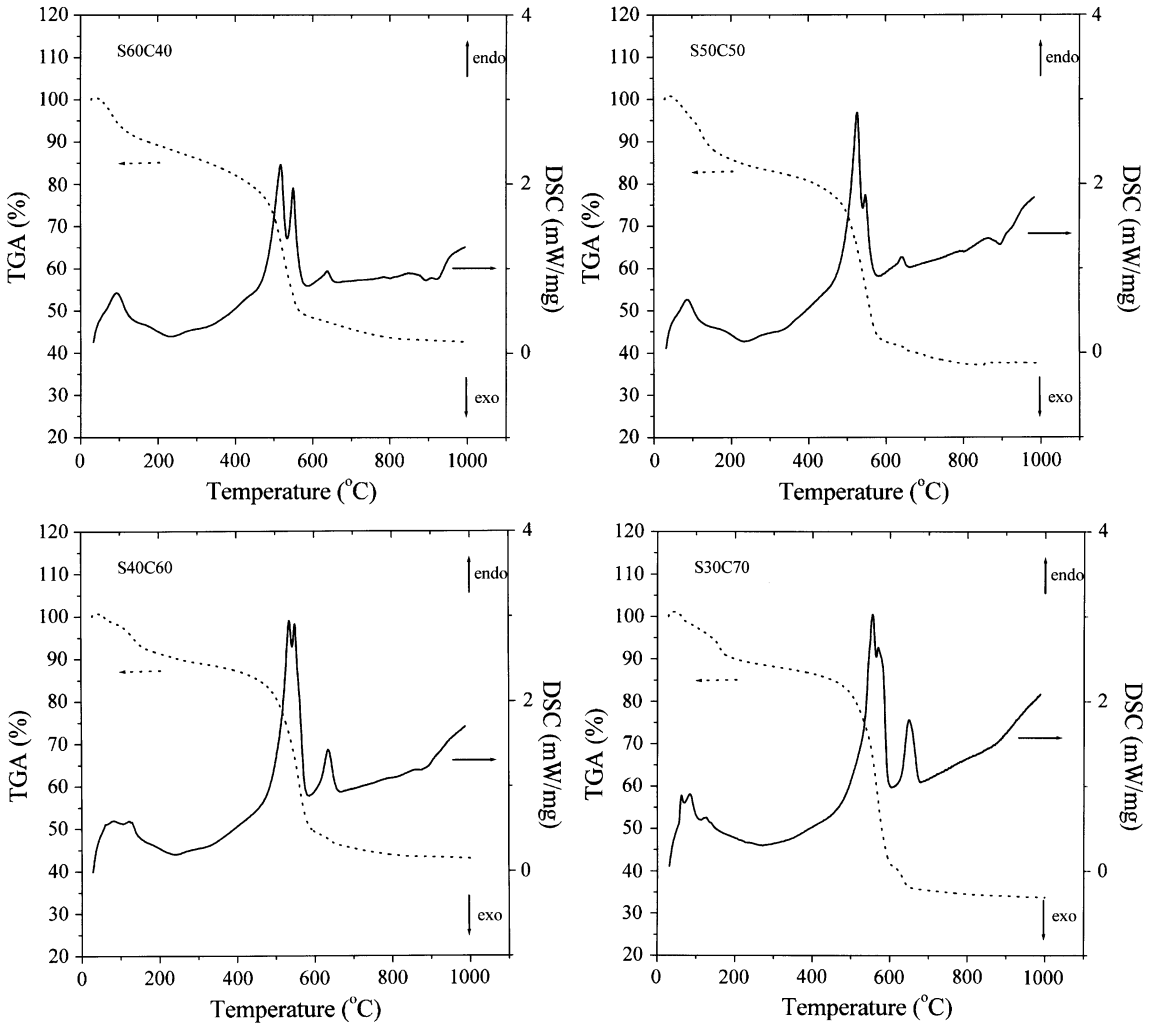

Fig. 1 TGA-DSC traces for S60C40, S50C50, S40C60 and S30C70 gel powders that have been dried at 120°C

became more compact than the corresponding cements without gelatin.

3.6 Anti-washout properties

Washout resistance results are shown in the photo in Fig. 5. The picture was taken 60 min after the cement specimens were immersed in SBF. The four controls appeared to degrade after immersion. It can clearly be seen that the gelatin hybrid cements resisted washout, showing no noticeable breakdown.

3.7 Setting time

After mixing with water, the control cements set in the range of 10–29 min, which were shortened with an increase in the concentration of the calcium component, as shown in Fig. 6. These values were significantly ($P < 0.05$) different from each other. Scheffe's multiple comparison testing revealed no significant difference ($P > 0.05$) between S30C70 and S40C60. It was also not significant different ($P > 0.05$) for the S50C50 and S60C40 control. The addition of 5% and 10% gelatin significantly ($P < 0.05$) prolonged the setting time of the hybrid cements by a factor of about 2 (25–69 min) and 8 (108–282 min), respectively. In the case of CSCs containing either 5% or 10% gelatin content, setting time had significant differences ($P < 0.05$) between various CSCs.

3.8 Diametral tensile strength and modulus

Figure 7 illustrates typical diametral tensile stress–strain curves for S50C50 with and without 5% and 10% gelatin. The three curves were different in shape after the force was applied. The control showed a typical "brittle" fracture, which was initially elongated in an elastic (linear) way, followed by abrupt failure. In the case of gelatin, elastic

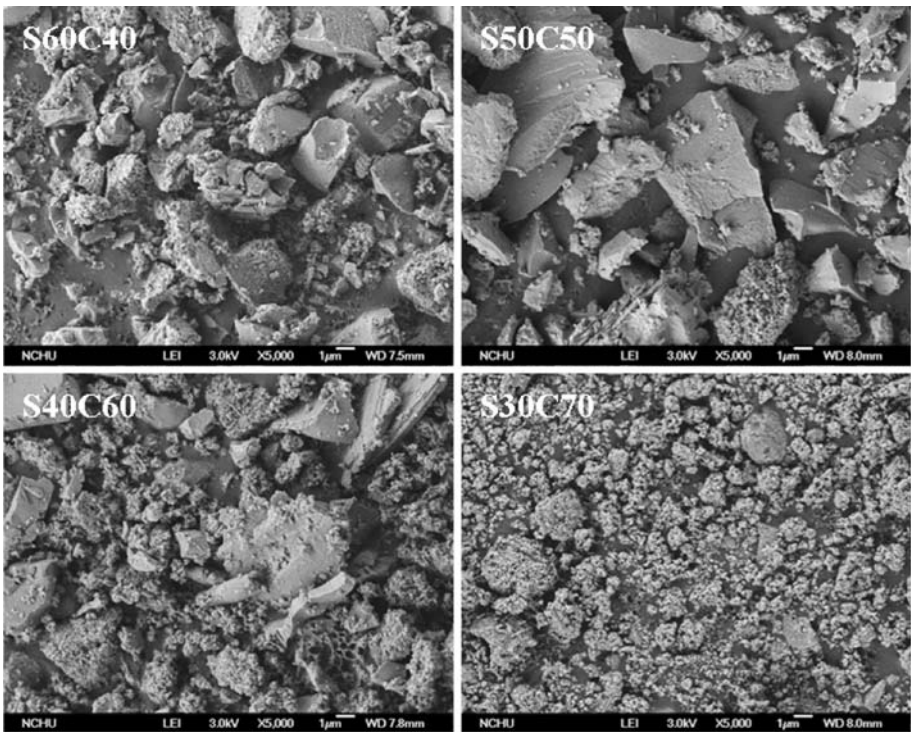

Fig. 2 SEM micrographs of various ground powders sintered at 800°C

deformation followed an initial non-linear region. After arriving at peak stress, the strain continued to completely fail. Figure 8 shows that the DTS values of the hardened control cements were 2.0, 2.6, 2.0, and 1.0 MPa with an increasing CaO content, indicating there was a significant difference ($P < 0.05$). The incorporation of gelatin into the CSC did not significantly affect ($P > 0.05$) its strength, which was comparable to that of the control cement. In the case of S40C60 group, the DTS values were 2.0, 2.1, and 1.7 MPa for 0, 5, 10% gelatin content, respectively. The significant differences ($P < 0.05$) in DTS between S40C60 and S60C40 groups were not found. On the other hand, Scheffe's multiple comparison testing indicated that both 5% and 10% gelatin-containing S50C50 cement specimens had significantly ($P < 0.05$) higher DTS values than the other CSC systems with and without gelatin, with the exception of the S50C50 control.

The values of the mean elastic moduli obtained during the measurement of diametral tensile strength are shown in Fig. 9 along with the respective standard deviations. The elastic moduli of the CSC systems with and without gelatin in the range of 26.8–43.3 MPa presented significant differences ($P < 0.05$). It was found that the S50C50 control had an insignificantly higher modulus than the other three CSC controls ($P > 0.05$). The modulus decreased somewhat after the incorporation of either 5% or 10% gelatin to the CSC control, but there was not significantly different ($P > 0.05$) for the same CSC system after Scheffe's multiple comparison testing.

3.9 Fracture analysis

Figure 10 shows the interior surface of the set cement specimens with and without 10% gelatin after diametral tensile loading. The fractured surfaces of the S30C70 cement presented a smoother structure when compared to those with lower CaO contents in the cement. In contrast to the control cements, there were seemingly more pores present inside of gelatin-containing cement specimens, which might be due to the leaching of gelatin gel.

4 Discussion

TGA and DSC were used to define the sintering temperatures of the as-prepared SiO_2−CaO gel specimens (Fig. 1). All powder specimens indicated a first weight loss of about 10%, where a broad endotherm was observed at around 100°C. This was due to evaporation of residual or absorbed solvent [3], pore liquid [3, 20] and crystalline water in the $Ca(NO_3)_2{\cdot}4H_2O$ precursor [21]. The continuous weight loss from 100 to 450°C was suggested to be due to the decomposition of organic species produced from hydrolysis/condensation reactions, which are accelerated at 400–550°C, as evidenced by rapid weight loss of more than 30% in this temperature range. There was no appreciable weight loss observed above 700°C, indicating that the precursors may generate a phase after heat-treatment at temperatures more than 700°C. In the DSC curves, the endothermic

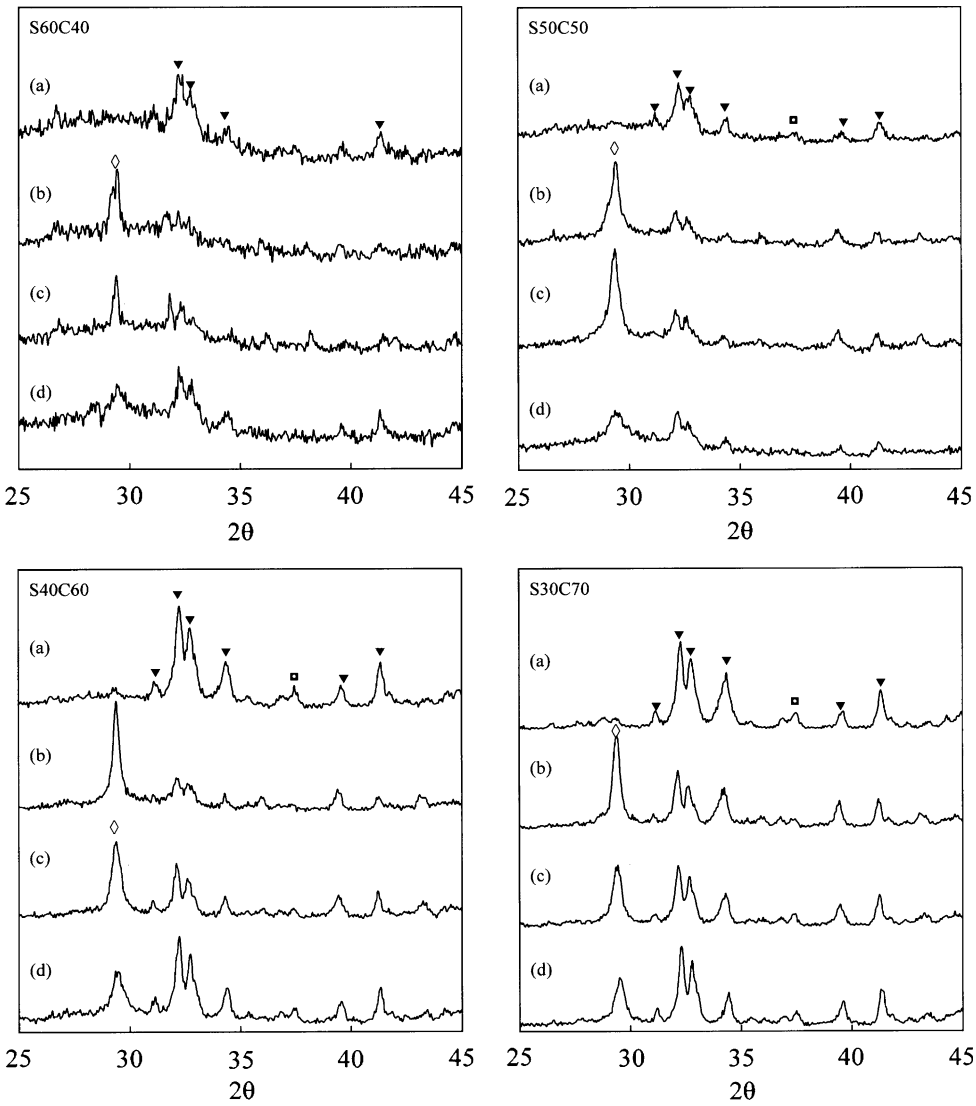

Fig. 3 XRD patterns of the four CSC systems.(*a*) Powder, (*b*) cement without gelatin, (*c*) cement containing 5 wt% gelatin, and (*d*) cement containing 10 wt% gelatin. ◘: CaO; ▼: β-Ca_2SiO_4; ◇: C–S–H

peaks in the range of 520–540°C were caused by the condensation of silanol groups and the release of nitrate groups introduced as calcium nitrate in the preparation of the sol [3, 20], which was consistent with the results of the TGA. The endothermic peak around 650°C was ascribed to the chemical reactions between the precursors, which may lead to the formation of a crystalline phase. The band intensity increased with increasing CaO content in the sol, as confirmed by XRD analysis (Fig. 3). The exothermic maximum at about 900°C, with the exception of S30C70, could possibly be due to the crystallization of a calcium silicate phase. Based on the TGA-DSC data, thermal treatment at 800°C for 2 h in air was used to prepare the SiO_2−CaO powders.

When the ratio of components within the cement powder was altered, its physical properties changed accordingly. Concerning morphology (Fig. 2), although the sinter-granulated powder was irregularly-shaped, it had a different morphology. It is noteworthy that the S30C70 power was seemingly easier fragile than the other three powders under the same milling condition, which may affect the mechanical strength of the cement. In contrast to those with lower SiO_2 amounts (S40C60 and S30C70), the powders with higher SiO_2 (S60C40) tended to have a denser structure and larger particle size. This is possibly because of a SiO_2-induced liquid phase sintering effect, where SiO_2 acts as a sintering aid [22]. The present XRD results seemed to support this deduction, namely, S60C40 was a poorly crystalline powder containing a great amount of the amorphous SiO_2 phase. The increased β-Ca_2SiO_4 and CaO amounts of sintered powders, with an increase in the CaO content of the starting materials, may be interpreted by the product of the decomposition of calcium nitrate that remained either partially reacted or unreacted in the gel after heat treatment. To further confirm the phase evolution, the related crystallinity (or amount of β-Ca_2SiO_4 phase) of

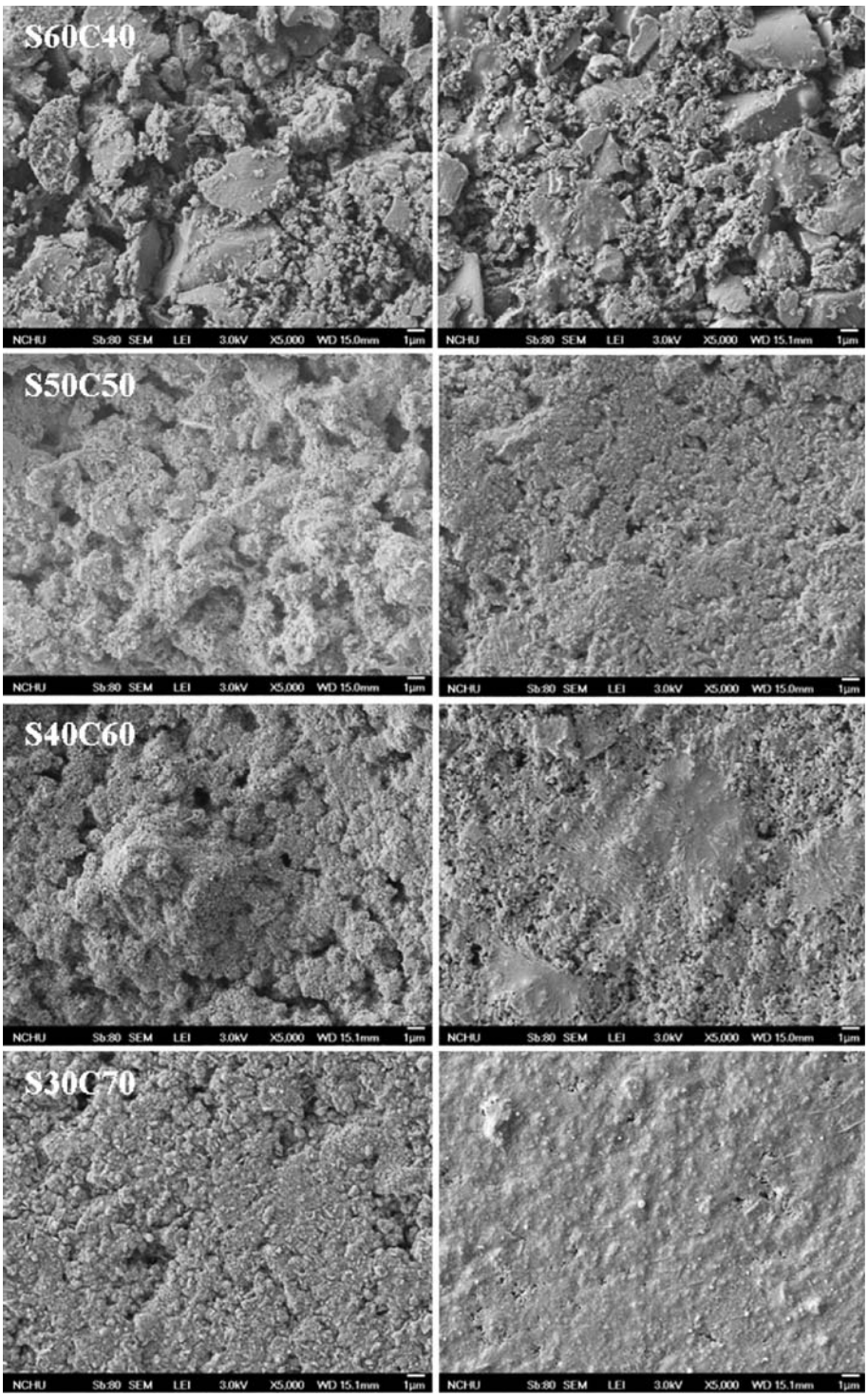

Fig. 4 Surface SEM micrographs of various cements with (*right*) and without (*left*) 10 wt% gelatin

the powders was calculated based on the integrated area under two major peaks of (103) and (200) at $2\theta = 32.2$ and 32.7°, respectively. It shows that amount of β-Ca_2SiO_4 phase of S30C70, S40C60 and S50C50 was about 3.2, 2.8, and 1.4 fold, respectively, greater than that of the S60C40 powder. This indicated that calcium was a promoter of the crystallinity in the SiO_2-CaO system, which in turn, shortening the setting time.

For each of the cement types, there were appreciable differences in the composition and crystalline structure between the powder and set form. After mixing with water, β-Ca_2SiO_4 reacted with water to form C–S–H (Fig. 3). The

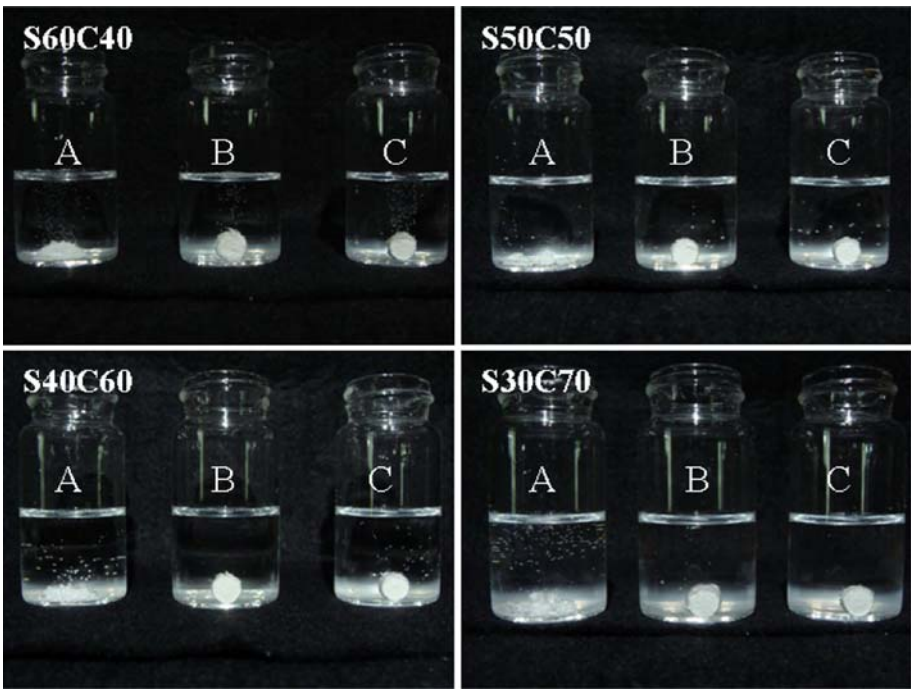

Fig. 5 Anti-washout properties of the four cements. (*A*) The control, (*B*) 5% gelatin-containing, and (*C*) 10% gelatin-containing cements. Immediately after mixing, the cement bulks was immersed in SBF. The picture was taken 60 min later

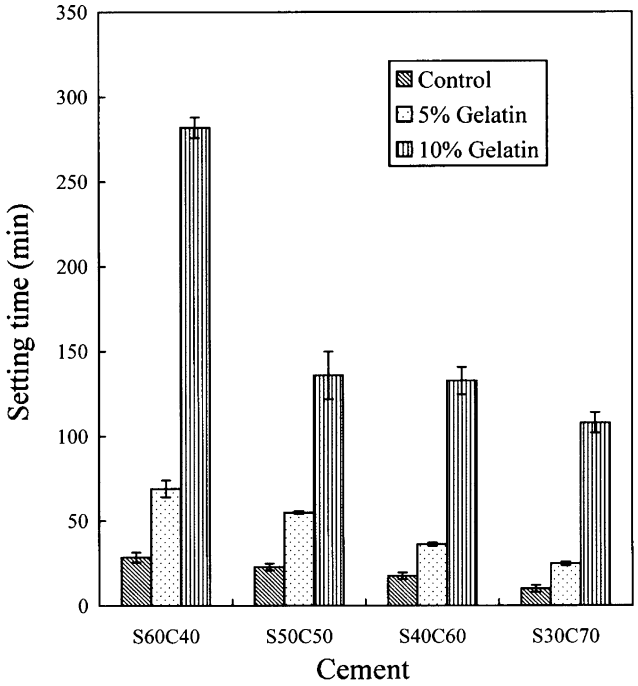

Fig. 6 Setting time of various cements with and without gelatin

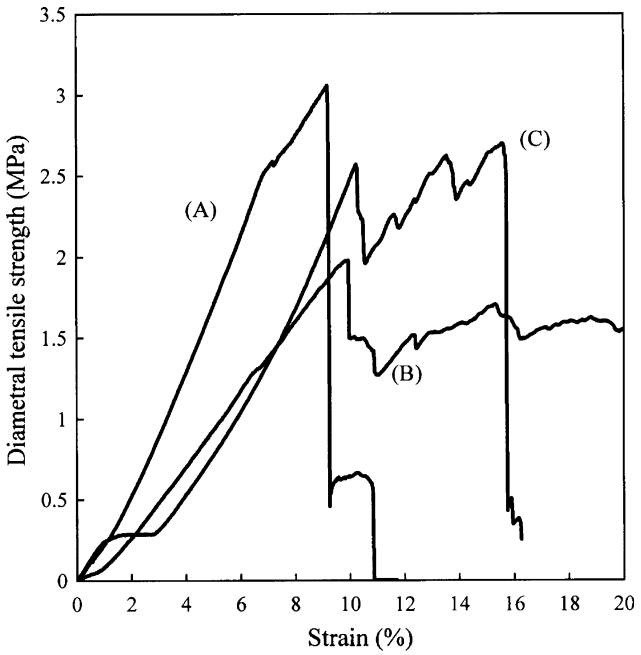

Fig. 7 Representative stress–strain curves of the hardened S50C50 cements measured by diametral tensile test. (*A*) The control, (*B*) 5% gelatin-containing, and (*C*) 10% gelatin-containing cements

principal setting process of the present powder was initiated on contact with water, when a chemical reaction between water and cement began; this was essentially a hydration reaction, similar to that in Portland cement [23]. Cement hydration connected the originally hydrophilic particles together (Fig. 4), resulting in a C–S–H gel that developed bonding properties and was responsible for its hardening [24].

The added gelatin, which was examined in this study, may play a crucial role in the properties of the hybrid cements. A colloidal gel formed a dense structure of hydrated hybrid cement that entanged the original C–S–H structure. Such a dense structure of gelatin-containing cements might be due to the existence of negatively charged gelatin. Type B gelatin with an isoselectric point

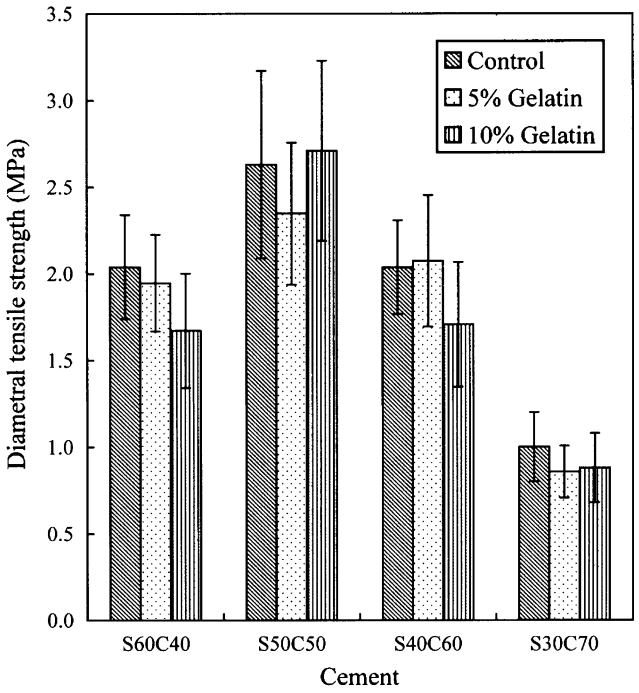

Fig. 8 DTS of various CSCs with and without gelatin

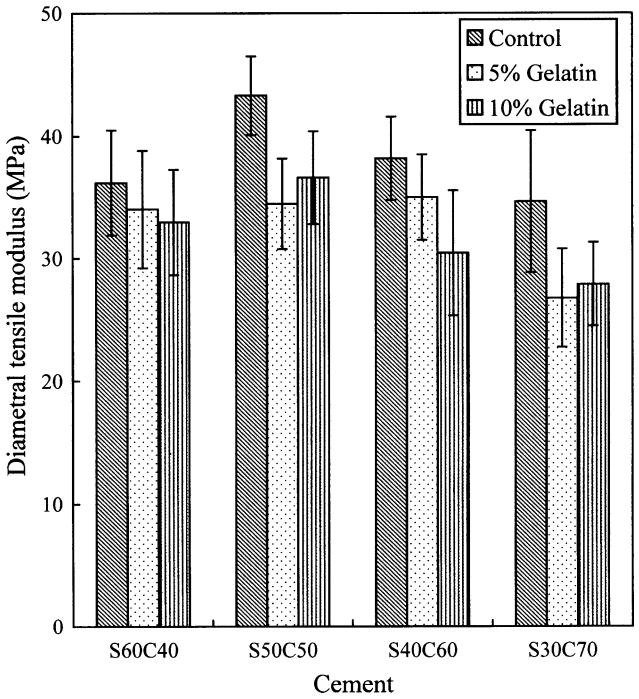

Fig. 9 Diametral tensile modulus of various CSCs with and without gelatin

of about 5 has a high density of carboxyl groups, which makes the gelatin negatively charged [25]. The carboxyl groups might bind calcium ions on the surface of calcium silicate particles. Hence, more entanglements were formed between the inorganic particles and concrete cement bodies; this finding was similar to another study [26]. The enhanced structure may improve the washout and brittle properties of the CSC. On the other hand, the reaction could inhibit C–S–H formation. This might explain why the presence of gelatin in the cement specimen apparently reduced the peak intensity of C–S–H at $2\theta = 29.4°$ (Fig. 3) and prolonged the setting time (Fig. 6).

Cement washout can occur in vivo when it comes in contact with physiological fluids or when bleeding occurs due to difficulty in achieving complete hemostasis [7]. The paste of the four control cements could be washed out completely when immersed in SBF immediately after mixing. In contrast, the gelatin hybrid cements resisted washout (Fig. 5). Although the detailed mechanisms of washout resistance for gelatin-containing CSCs have not been fully clarified at present, the improvement in anti-washout properties can be attributed to the adhesive property and negative charge of gelatin, which serves as a 'glue' to fuse the particles together, as confirmed by SEM. The physical reaction may prohibit the penetration of cement paste by liquid, which is considered a cause of the washing out properties of cement pastes [6, 27], thus endowing the gelatin-containing CSCs with anti-washout ability. The polymeric gelatin materials have the potential to improve the anti-washout properties of CSCs.

Calcium silicate cement consists of a powder containing one or more solid compounds of calcium silicate and a liquid phase that can be water or an aqueous solution [5]. The setting time is one of the most clinically relevant factors. A long setting duration could cause clinical problems due to the cement's inability to maintain shape and support stress during this period [7]. When water was used as a liquid phase, the setting time of the control cement was in the range of 10–29 min, much lower than the results obtained by the Chang group [28, 29]. They developed sol–gel-derived tricalcium silicate and dicalcium silicate cements that had initial setting times of over 1 h. The differences may reside in the powder preparation and chemical composition. In the present study, the setting time was significantly inverse proportional to Si/Ca ratio. With an increase in the concentration of the calcium component, the setting time of the cement became shorter, reaching 10 min (S30C70) from 29 min (S60C40), demonstrating the acceleration role of calcium in the setting reaction. This result may be interpreted by the amount (or crystallinity) of the β-Ca_2SiO_4 phase that could affect the formation of C–S–H gel. It is speculated that the set product was related to the hardening mechanism of the present CSCs. Higher C–S–H content in the final hydrated product yielded a better and faster hydration reaction, leading to a shorter setting time.

As to the gelatin effect, the addition of 5% and 10% gelatin prolonged the setting time of the hybrid cement by

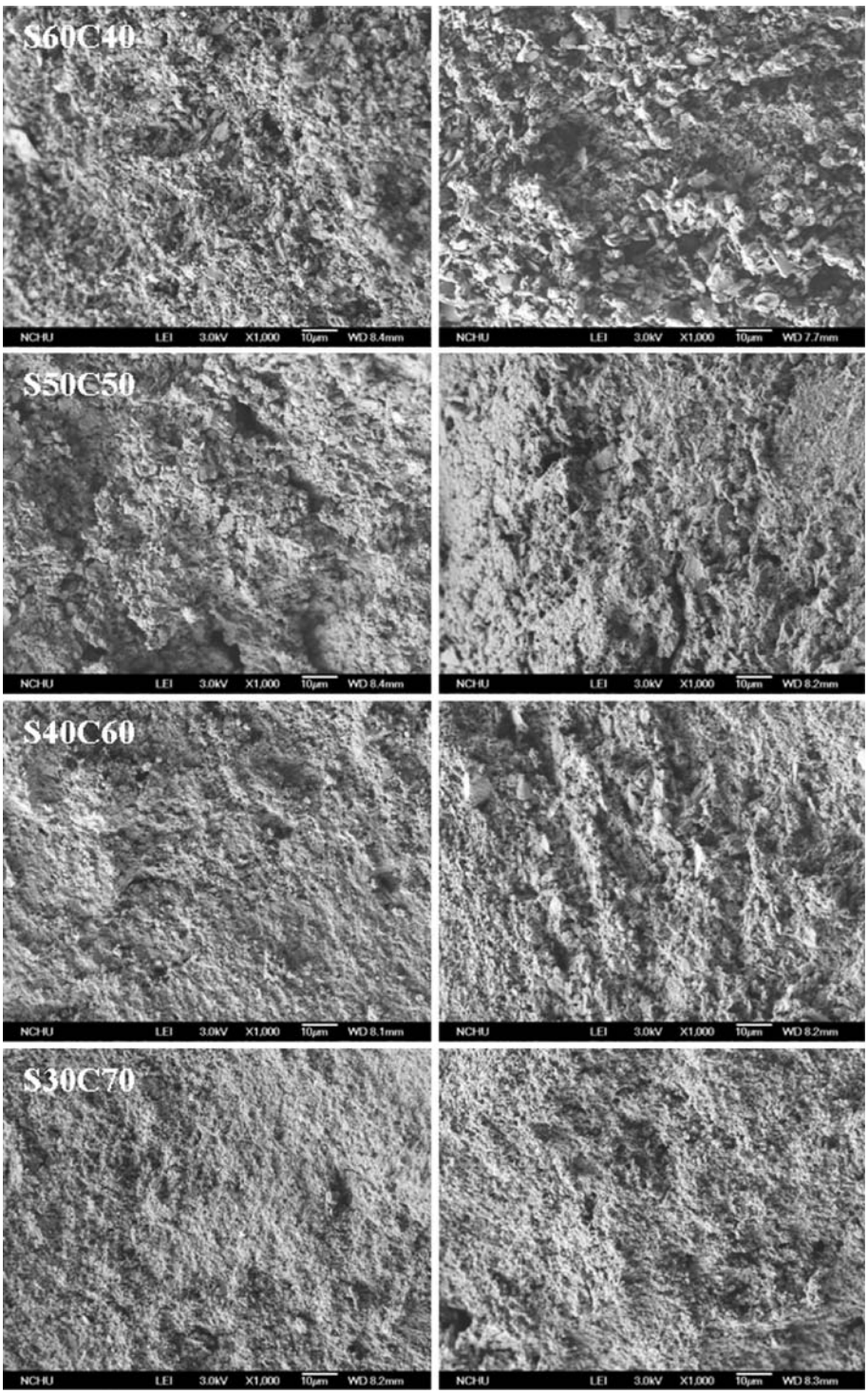

Fig. 10 SEM micrographs of the fractures surfaces of various cements with (*right*) and without (*left*) 10 wt% gelatin

up to about 2 and 8 times, respectively, indicating the adverse effect of gelatin on the hardening reaction of CSCs. For example, S50C50 had setting times of 55 and 136 min when containing 5% and 10% gelatin, respectively, from the original 23 min of the control without gelatin. Naturally polymeric gelatin absorbs the water and forms a gel that partially encapsulates the particles and impedes the hydration reaction of the CSC. The resulting hardening properties of the hybrid cements would be a combination between the progressive hardening due to the main calcium silicate reactant and the progressive complex reaction, such as intramolecular hydrogen bonding between water and the gelatin phase. Wang et al. reported that excessive polyanions destroy the balance of cement

components within a ceramic cement, leading to very slow setting processes or no setting at all [30]. Polymer interactions with cement and their contributions to the hydration reaction are far from being clarified and deserve further investigation, despite the evident importance of additives.

The four CSC systems could give C–S–H as the final product after their powder phases were mixed with water. However, their DTS results were significantly different ($P < 0.05$); for example, 2.6 MPa for S50C50 and 1.0 MPa for the fastest setting S30C70. These values were also greater than the applied pressure of 0.7 MPa that was used to prepare the cement specimen. 0.7 MPa is a commonly-used compaction pressure based on the suggestion of Chow's group [31]. This was because most clinical situations allowed the application of a small pressure to push the cement into the bone defects. Hence, it was reasonably deduced that the applied pressure did not affect the DTS values and washout properties, in agreement with the previous study [32]. Although the detailed mechanism underlying the changes in DTS has not been fully clarified, it seemed that at least two factors, i.e. a formed C–S–H and remaining reacted phase structure, were operating competitively to determine the eventual strength level of the four cements. XRD patterns also indicated that there were incompletely reacted inorganic component phases of β-Ca_2SiO_4 in the set cement specimen, in addition to hydration product of C–S–H (Fig. 3). The interlinking or entanglement between the set products was thought to be responsible for the mechanical strength of the cements [33]. Nevertheless, the denser and quickest-setting S30C70 cement had the lowest strength among the four control groups possibly due to weak cohesion within unreacted microstructure, as indicated in particle morphology with a fragile type (Fig. 1), which might lead to an intragranular fracture (Fig. 10).

The stress–strain measurement results in Fig. 7 show that blending with gelatin significantly changes the mechanical properties, including the inelastic deformation and breaking strain of CSCs. As expected, specimens of the pure cement exhibited inherently low ductility in the ceramics. In contrast, the resulting stress–strain curves of the gelatin-containing CSCs were similar to the tensile behavior observed in mechanical tests of a demineralized bovine cortical bone specimen [34], exhibiting an initial non-linear 'toe' region, followed by a linear region and subsequent failure. Gelatin is an elastic polymer consisting of the amorphous components. The amorphous phase of the cement specimens during the stretching could be reorienting up to breakage. The interaction between the gelatin additive and calcium silicate matrix can impact the level of reinforcement. Enhanced ductility was achieved when the small organic molecules were uniformly dispersed throughout the ceramics and interacted strongly with the ceramic matrix. The increasing gelatin content did increase the ductility of CSC, while the mean fracture strength and modulus showed only small changes with no significant differences ($P > 0.05$). For example, the highest DTS value was 2.6 MPa, which belonged to the cement of CaO/$SiO_2 = 1$, whose value changed to 2.4 and 2.7 MPa when adding 5% and 10% gelatin, respectively. On the other hand, the values of the mean elastic moduli were 43.3, 34.5, and 36.6 MPa for the control, 5%, and 10% gelatin-containing cements, respectively, indicating no differences were found ($P > 0.05$).

The novel washout-resistant bone cements composed of gelatin and calcium silicate have successfully developed. However, the setting time of gelatin-containing cements may be improved in term of clinical applications. Additionally, the poor mechanical properties reduced a wider clinical application of the hybrid cements. Another disadvantage of the present cement was its lack of macropores that can promote biodegradation and bioresorption. For some clinical applications, such as periodontal bone defects repair, sinus lift, etc., the ability of the hardened cement to be replaced quickly by bone was crucial [35].

5 Conclusions

The present study, to the best of our knowledge, is the first work on the development of anti-washout-type gelatin-containing CSCs. Upon combining gelatin with calcium silicate, a significant modification was observed in the external aspects of the cements—a more compact structure. In contrast to the cements without gelatin, setting times ranging from 10 to 29 min significantly increased to values of 25–69 min of 5 wt% gelatin cements, and decreased with an increasing CaO content in the sol. However, the added gelatin was effective at improving the washout properties of CSCs. The incorporation of gelatin did not significantly influence the diametral tensile strength, but enhanced the ductility of CSCs. Although the addition of 5 wt% gelatin prolonged the setting time by a factor of about 2, this prolonged setting time may be acceptable. Taking the mechanical strength and anti-washout properties into account, the S50C50 cement with 5 wt% gelatin may be the best choice among the hybrid CSC systems. The novel anti-washout-type gelatin-containing CSCs may be promising for use in dental, craniofacial and orthopedic repair. Additional studies, including in vitro bioactivity and biocompatibility tests, are currently underway to evaluate the clinical potential of the hybrid CSCs.

Acknowledgements The authors acknowledge with appreciation the support of this research by the National Science Council of the Republic of China under the grant No. NSC 97-2320-B-040-001-MY2.

References

1. Siriphannon P, Kameshima Y, Yasumori A, Okada K, Hayashi S. Influence of preparation conditions on the microstructure and bioactivity of α-$CaSiO_3$ ceramics: formation of hydroxyapatite in simulated body fluid. J Biomed Mater Res. 2000;52:30–9.
2. Sarmento C, Luklinska ZB, Brown L, Anseau M, De Aza PN, De Aza S. In vitro behavior of osteoblastic cells cultured in the presence of pseudowollastonite ceramic. J Biomed Mater Res A. 2004;69:351–8.
3. Izquierdo-Barba I, Salinas AJ, Vallet-Regí M. In vitro calcium phosphate layer formation on sol-gel glasses of the $CaO–SiO_2$ system. J Biomed Mater Res. 1999;47:243–50.
4. Kao CT, Shie MY, Huang TH, Ding SJ. Properties of an accelerated mineral trioxide aggregate-like root-end filling material. J Endod. 2009;35:239–42.
5. Ding SJ, Shie MY, Wang CY. Novel fast-setting calcium silicate bone cements with high bioactivity and enhanced osteogenesis in vitro. J Mater Chem. 2009;19:1183–90.
6. Wang X, Chen L, Xiang H, Ye J. Influence of anti-washout agents on the rheological properties and injectability of a calcium phosphate cement. J Biomed Mater Res B. 2007;81:410–8.
7. Ishikawa K, Miyamoto Y, Takechi M, Toh T, Kon M, Nagayama M, et al. Non-decay type fast-setting calcium phosphate cement: hydroxyapatite putty containing an increased amount of sodium alginate. J Biomed Mater Res. 1997;36:393–9.
8. Ito M, Yamagishi T, Yagasaki H, Kafrawy AH. In vitro properties of a chitosan-bonded bone-filling paste: studies on solubility of calcium phosphate compounds. J Biomed Mater Res. 1996;32:95–8.
9. Fujishiro Y, Takahashi K, Sato T. Preparation and compressive strength of α-tricalcium phosphate/gelatin gel composite cement. J Biomed Mater Res. 2001;54:525–30.
10. Panzavolta S, Fini M, Nicoletti A, Bracci B, Rubini K, Giardino R, et al. Porous composite scaffolds based on gelatin and partially hydrolyzed α-tricalcium phosphate. Acta Biomater. 2009;5:636–43.
11. Khairoun I, Driessens FCM, Boltong MG, Planell JA, Wenz R. Addition of cohesion promotors to calcium phosphate cements. Biomaterials. 1999;20:393–8.
12. Cherng A, Takagi S, Chow LC. Effects of hydroxypropyl methylcellulose and other gelling agents on the handling properties of calcium phosphate cement. J Biomed Mater Res. 1997;35:273–7.
13. Olsen D, Yang C, Bodo M, Chang R, Leigh S, Baez J, et al. Recombinant collagen and gelatin for drug delivery. Adv Drug Delivery Rev. 2003;55:1547–67.
14. Fratzl P, Gupta HS, Paschalis EP, Roschger P. Structure and mechanical quality of the collagen–mineral nano-composite in bone. J Mater Chem. 2004;14:2115–23.
15. Shie MY, Chen CH, Wang CY, Chiang TY, Ding SJ. Immersion behavior of gelatin-containing calcium phosphate cement. Acta Biomater. 2008;4:646–55.
16. Ding SJ. Preparation and properties of chitosan/calcium phosphate composites for bone repair. Dent Mater J. 2006;25:706–12.
17. Pan Z, Jiang P, Fan Q, Ma B, Cai H. Mechanical and biocompatible influences of chitosan fiber and gelatin on calcium phosphate cement. J Biomed Mater Res B. 2007;82:246–52.
18. Xu HHK, Takagi S, Quinn JB, Chow LC. Fast-setting calcium phosphate scaffolds with tailored macropore formation rates for bone regeneration. J Biomed Mater Res A. 2004;68:725–34.
19. ISO 9917-1, Dentistry-water-based cements part 1: powder/liquid acid-base cements. International Standard Organization; 2003.
20. Jones JR, Ehrenfried LM, Hench LL. Optimising bioactive glass scaffolds for bone tissue engineering. Biomaterials. 2006;27:964–73.
21. Kim IS, Kumta PN. Sol-gel synthesis and characterization of nanostructured hydroxyapatite powder. Mater Sci Eng B. 2004;111:232–6.
22. Ikesue A, Yoshida K, Yamamoto T, Yamaga I. Optical scattering centers in polycrystalline Nd:YAG Laser. J Am Ceram Soc. 1997;80:1517–22.
23. Older I. Hydration, setting and hardening of Portand cement. In: Hewlett PC, editor. Lea's chemistry of cement and concrete. 4th ed. Oxford: Butterworth-Heinemann; 2007. p. 241–97.
24. Bentz DP. Cement hydration: building bridges and dams at the microstructure level. Mater Struct. 2007;40:397–404.
25. Tabata Y, Ikada Y. Protein release from gelatin matrices. Adv Drug Deliv Rev. 1998;31:287–301.
26. Wang XH, Ma JB, Wang Y, He BL. Structural characterization of phosphorylated chitosan and their applications as effective additives of calcium phosphate cements. Biomaterials. 2001;22:2247–55.
27. Takechi M, Miyamoto Y, Ishikawa K, Yuasa M, Nagayama M, Kon M, et al. Non-decay type fast-setting calcium phosphate cement using chitosan. J Mater Sci: Mater Med. 1996;7:317–22.
28. Zhao W, Wang J, Zhai W, Wang Z, Chang J. The self-setting properties and in vitro bioactivity of tricalcium silicate. Biomaterials. 2005;26:6113–21.
29. Gou Z, Chang J, Zhai W, Wang J. Study on the self-setting property and the *in vitro* bioactivity of β-Ca_2SiO_4. J Biomed Mater Res B. 2005;73:244–51.
30. Wang XH, Feng QL, Cui FZ, Ma JB. The effects of S-chitosan on the physical properties of calcium phosphate cements. J Bioact Compat Polym. 2003;18:45–57.
31. Fukase Y, Eanes ED, Takagi S, Chow LC, Brown WE. Setting reactions and compressive strengths of calcium phosphate cements. J Dent Res. 1990;69:1852–6.
32. Chow LC, Hirayama S, Takagi S, Parry E. Diametral tensile strength and compressive strength of a calcium phosphate cement: effect of applied pressure. J Biomed Mater Res. 2000;53:511–7.
33. Ginebra MP, Fernandez E, De Maeyer EAP, Verbeeck RMH, Boltong MG, Ginebra J, et al. Setting reaction and hardening of an apatite calcium phosphate cement. J Dent Res. 1997;76:905–12.
34. Bowman SM, Zeind J, Gibson LJ, Hayes WC, McMahon TA. The tensile behavior of demineralized bovine cortical bone. J Biomech. 1996;29:1497–501.
35. Dorozhkin SV. Calcium orthophosphate cements for biomedical application. J Mater Sci. 2008;43:3028–57.